Analysis of Nonlinear System Response to an Impulse Excitation

G. Manson, K. Worden & P.I. Reed

University of Sheffield
Department of Mechanical Engineering, Mappin Street, S1 3JD
email: graeme.manson@sheffield.ac.uk

Abstract

The paper investigates the use of a Volterra series-based approach to explain the impulse response behaviour of nonlinear systems. Analytical expressions are derived using a frequency-domain based approach with the contour integration being conducted using the calculus of residues. The complexity of the process and the resulting expressions increases dramatically as the order of the response component increases and, for this reason, the work only considers the linear component of the impulse response and the first two nonlinear Volterra series components. The effect of including these components is then investigated by comparing the impulse responses from the Volterra expressions to the impulse response of a simulated single degree of freedom Duffing oscillator system. It is found that these components are capable of drastically decreasing the error when compared with the linear impulse response but, at higher forcing levels, the Volterra approach can suffer from convergence problems which may result in worse predictions than the linear response.

Key words: Nonlinear Systems, Impulse Response, Volterra Series, Duffing Oscillator, Polynomial Nonlinearity

1 Introduction

The current work adopts a Volterra series approach to attempt to better understand the the behaviour of nonlinear systems when an impulse excitation is applied and is the latest in an ongoing series of papers [1, 2, 3] which attempt to extend the understanding of structural dynamics observables using the Volterra functional series approximation of nonlinear system behaviour.

There do not appear to have been many investigations in the literature regarding the development of analytical expressions for impulse responses of nonlinear systems. White [4] considered a perturbation analysis approach to explain the first nonlinear component of the impulse response of a system with cubic nonlinear stiffness but was unable to obtain good agreement with simulation. Mohammad [5] considered both perturbation and Volterra time-domain-based approaches to develop expressions for the impulse response for a system with quadratic stiffness but there appear to have been errors with the analysis and no validation results were presented.

Throughout this work it is assumed that the Volterra series representation exists for the systems. Sufficient conditions for this requirement are known [6] [7]. Essentially, it is required that the system nonlinearity be analytic. Another restriction is that the nonlinear system must have finite memory. Essentially this means that the system will reach a steady-state condition not governed by the initial conditions. This requirement precludes the use of the Volterra series for hysteretic systems and systems with limit cycles. Of greater concern is the issue of convergence. The Volterra series, being a functional form of the Taylor series, suffers similar limitations [8] and this will be briefly addressed when discussing the results in Section 5.

2 Impulse response of a linear system

Calculating the response of a linear system to an impulse excitation is straightforward if one adopts an impulse-momentum approach. Consider a linear single degree of freedom (SDOF) system whose equation

of motion is given by

$$m\ddot{y}(t) + c\dot{y}(t) + ky(t) = x(t) \tag{1}$$

and where m represents mass, c, viscous damping, and k, linear spring stiffness. The response of the system, $y(t)$, to an impulse excitation, $x(t) = A\delta(t)$, where $\delta(t)$ is the Dirac delta function, will be equal to

$$y(t) = Ah(t) = \frac{A}{m\omega_d} e^{-\zeta\omega_n t} \sin(\omega_d t) \tag{2}$$

where $h(t)$ is known as the impulse response function of the system. This is usually the first step in the development of the convolution or Duhamel integral.

An alternative approach for calculating the impulse response of a linear system is offered by considering the problem in the frequency domain and applying the calculus of residues. Whilst this may appear a very roundabout method for the linear system, it will be the foundation for the calculation of the impulse response of nonlinear systems which will be considered in the following sections. Rewriting equation (2) using the frequency response function, $H(\omega)$ gives

$$y(t) = Ah(t) = \frac{A}{2\pi} \int_{-\infty}^{+\infty} d\omega \; H(\omega) \; e^{i\omega t} \tag{3}$$

where the frequency response function, $H(\omega)$, of the SDOF linear system of equation (1) is given by

$$H(\omega) = \frac{1}{-\omega^2 m + i\omega c + k} = \frac{1}{-m(\omega - p_1)(\omega - p_2)} \qquad p_{1,2} = \pm\omega_d + i\zeta\omega_n \tag{4}$$

Substituting equation (4) into equation (3) gives the following expression for the system response:

$$y(t) = -\frac{A}{2\pi m} \int_{-\infty}^{+\infty} d\omega \frac{e^{i\omega t}}{(\omega - p_1)(\omega - p_2)} \tag{5}$$

The integral can be evaluated using the contour integral method. This approach is well-known and details can be found in many textbooks such as [9]. Essentially, it can be shown that, if a contour is closed in a counterclockwise path on half of the complex plane with poles α_j included inside the contour, the integral, I, is given by

$$I = 2\pi i \sum_j \text{res } \alpha_j \tag{6}$$

when the contour is closed on the upper-half of the plane and

$$I = -2\pi i \sum_j \text{res } \alpha_j \tag{7}$$

when it is closed on the lower-half of the plane [1]. The term res α_j is the residue at the pole α_j and is defined for a simple pole as

$$\text{res } \alpha_j = \lim_{z \to \alpha_j} [(z - \alpha_j) f(z)] \tag{8}$$

Letting α_1 correspond to p_1 and α_2 to p_2 and adopting the previous equation, results in the following two residues for the integral of equation (5):

$$\text{residue at } \alpha_1 = \frac{e^{ip_1 t}}{(p_1 - p_2)} \qquad \text{residue at } \alpha_2 = \frac{e^{ip_2 t}}{(p_2 - p_1)} \tag{9}$$

Substituting equation (9) into equation (6) and using the expressions in equation (4) for the poles p_1 and p_2 gives an expression for the integral of equation (5). After a little tidying up this will eventually result in the same expression as that given in equation (2) from the impulse-momentum balance:

$$y(t) = -\frac{A}{2\pi m} \frac{2\pi i}{(p_1 - p_2)} \left(e^{ip_1 t} - e^{ip_2 t} \right) = \frac{A}{m\omega_d} e^{-\zeta\omega_n t} \sin(\omega_d t) \tag{10}$$

In the following section, this frequency domain method will be extended for nonlinear systems through the use of the Volterra series to represent the nonlinear system response.

[1] Titchmarsh's theorem [10] states that, for causal responses such as the impulse response, all poles will exist in the upper-half plane and therefore, in this work, closure will only be conducted in the upper-half plane.

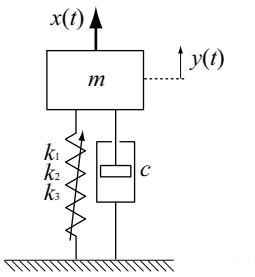

Fig. 1: Single degree of freedom (SDOF) nonlinear system

3 Volterra series representation of a nonlinear system

It is well-known that many nonlinear systems or input-output processes $x(t) \longrightarrow y(t)$ can be realised as a mapping [11] [12],

$$y(t) = y_1(t) + y_2(t) + y_3(t) + \ldots + y_n(t) + \ldots \tag{11}$$

where

$$y_n(t) = \int_{-\infty}^{+\infty} \ldots \int_{-\infty}^{+\infty} d\tau_1 \ldots d\tau_n \; h_n(\tau_1, \ldots, \tau_n) x(t-\tau_1) \ldots x(t-\tau_n) \tag{12}$$

This is the *Volterra series* and the functions h_n are the *Volterra kernels*. The dual frequency-domain representation is based on the *higher-order frequency response functions* (HFRFs) or *Volterra kernel transforms*, $H_n(\omega_1, \ldots, \omega_n)$, $n = 1, \ldots, \infty$, which are defined as the multi-dimensional Fourier transforms of the kernels. The dual time-frequency relationships are shown below:

$$H_n(\omega_1, \ldots, \omega_n) = \int_{-\infty}^{\infty} \ldots \int_{-\infty}^{\infty} d\tau_1 \ldots d\tau_n \; h_n(\tau_1, \ldots, \tau_n) e^{-i(\omega_1\tau_1 + \ldots + \omega_n\tau_n)}$$

$$h_n(\tau_1, \ldots, \tau_n) = \left(\frac{1}{2\pi}\right)^n \int_{-\infty}^{\infty} \ldots \int_{-\infty}^{\infty} d\omega_1 \ldots d\omega_n \; H_n(\omega_1, \ldots, \omega_n) e^{i(\omega_1\tau_1 + \ldots + \omega_n\tau_n)} \tag{13}$$

The system which will be studied here is the asymmetric Duffing oscillator, shown in Figure 1, with the following equation of motion:

$$m\ddot{y}(t) + c\dot{y}(t) + k_1 y(t) + k_2 y(t)^2 + k_3 y(t)^3 = x(t) \tag{14}$$

where m represents mass, c, viscous damping, k_1, the linear spring stiffness, k_2, the quadratic spring stiffness and k_3, the cubic spring stiffness.

For the following analysis, it will be necessary to determine expressions for the first three HFRFs and there are a number of methods for achieving this for a given system. If the equations of motion are available, the method of harmonic probing [13] is both simple and effective and is the method applied here. For the asymmetric Duffing oscillator, the first three HFRFs are given by,

$$H_1(\Omega) = \frac{1}{(k_1 - \Omega^2 m + i\Omega c)} \tag{15}$$

$$H_2(\Omega_1, \Omega_2) = -k_2 H_1(\Omega_1 + \Omega_2) H_1(\Omega_1) H_1(\Omega_2) \tag{16}$$

$$\begin{aligned} H_3(\Omega_1, \Omega_2, \Omega_3) = {} & H_1(\Omega_1 + \Omega_2 + \Omega_3) H_1(\Omega_1) H_1(\Omega_2) H_1(\Omega_3) \times \\ & \left\{ \frac{2}{3} k_2^2 \left[H_1(\Omega_1 + \Omega_2) + H_1(\Omega_1 + \Omega_3) + H_1(\Omega_2 + \Omega_3) \right] - k_3 \right\} \end{aligned} \tag{17}$$

4 Impulse response of a nonlinear system

In the present section, the alternative approach for the calculation of the impulse response of a linear system introduced in Section 2 will be extended using the Volterra Series which was introduced in Section 3.

The Volterra series response of a nonlinear system, $y(t)$, to an impulse excitation, $x(t) = A\delta(t)$, may be easily calculated by substituting the input into equation (12) and summing the contributions as in equation (11) to give:

$$y(t) = y_1(t)+y_2(t)+y_3(t)+\ldots+y_n(t)+\ldots = Ah_1(t)+A^2h_2(t,t)+A^3h_3(t,t,t)+\ldots+A^nh_n(t,\ldots,t)+\ldots \quad (18)$$

As with in Section 2 for the linear system, the impulse response of the nonlinear system will be calculated using the frequency domain expressions. Substituting the Volterra kernels in equation (18) for their frequency domain representations using the second expression in equation (13) yields the following expression for the Volterra series impulse response:

$$\begin{aligned} y(t) = &\left(\frac{A}{2\pi}\right)\int_{-\infty}^{\infty} d\omega\ H_1(\omega_1)\ e^{i\omega t} + \left(\frac{A}{2\pi}\right)^2\int_{-\infty}^{\infty}\int_{-\infty}^{\infty} d\omega_1 d\omega_2\ H_2(\omega_1,\omega_2)\ e^{i(\omega_1+\omega_2)t} \\ &+ \left(\frac{A}{2\pi}\right)^3\int_{-\infty}^{\infty}\int_{-\infty}^{\infty}\int_{-\infty}^{\infty} d\omega_1 d\omega_2 d\omega_3\ H_3(\omega_1,\omega_2,\omega_3)\ e^{i(\omega_1+\omega_2+\omega_3)t} + \ldots \\ &+ \left(\frac{A}{2\pi}\right)^n\int_{-\infty}^{\infty}\ldots\int_{-\infty}^{\infty} d\omega_1\ldots d\omega_n\ H_n(\omega_1,\ldots,\omega_n)\ e^{i(\omega_1+\ldots+\omega_n)t} + \ldots \end{aligned} \quad (19)$$

The system whose impulse response will now be calculated is the asymmetric Duffing oscillator which is shown in Figure 1 and whose behaviour is described by equation (14). It will be seen shortly that, even for this relatively simple nonlinear system, the expressions will rapidly increase in complexity and, therefore, only the first three components, $y_1(t)$, $y_2(t)$ and $y_3(t)$ will be considered here. The first impulse response component for this system $y_1(t)$ has already been calculated in in Section 2 as this component will simply be the impulse response of the underlying linear system:

$$y_1(t) = \frac{A}{m\omega_d}\exp^{-\zeta\omega_n t}\sin(\omega_d t) \quad (20)$$

The contribution to the overall impulse response of the $y_2(t)$ will now be calculated. The expression from equation (19) may be rewritten for the system of interest by substituting the expression for $H_2(\omega_1,\omega_2)$ for this system given in equation (16)

$$\begin{aligned} y_2(t) &= \left(\frac{A}{2\pi}\right)^2\int_{-\infty}^{\infty}\int_{-\infty}^{\infty} d\omega_1 d\omega_2\ H_2(\omega_1,\omega_2)\ e^{i(\omega_1+\omega_2)t} \\ &= -k_2\left(\frac{A}{2\pi}\right)^2\int_{-\infty}^{\infty}\int_{-\infty}^{\infty} d\omega_1 d\omega_2\ H_1(\omega_1+\omega_2)H_1(\omega_1)H_1(\omega_2)\ e^{i(\omega_1+\omega_2)t} \end{aligned} \quad (21)$$

Each of the three linear FRF H_1 expressions may be rewritten in terms of poles as in equation (4) which gives the following expression for the $y_2(t)$ component:

$$y_2(t) = \frac{k_2}{m^3}\left(\frac{A}{2\pi}\right)^2\int_{-\infty}^{\infty}\int_{-\infty}^{\infty}\frac{d\omega_1 d\omega_2\ e^{i(\omega_1+\omega_2)t}}{(\omega_1-p_1)(\omega_1-p_2)(\omega_2-p_1)(\omega_2-p_2)(\omega_1+\omega_2-p_1)(\omega_1+\omega_2-p_2)} \quad (22)$$

This may be split into two integrals: one involving terms all terms dependent upon ω_1 and the other involving terms only dependent upon ω_2:

$$y_2(t) = \frac{k_2}{m^3}\left(\frac{A}{2\pi}\right)^2\int_{-\infty}^{\infty}\frac{d\omega_1\ e^{i\omega_1 t}}{(\omega_1-p_1)(\omega_1-p_2)(\omega_1+\omega_2-p_1)(\omega_1+\omega_2-p_2)}\int_{-\infty}^{\infty}\frac{d\omega_2\ e^{i\omega_2 t}}{(\omega_2-p_1)(\omega_2-p_2)} \quad (23)$$

It may be observed that first integral in the above expression consists of four poles (all in the upper-half of the complex plane) at

$$p_1 = \omega_d + i\zeta\omega_n \qquad p_2 = -\omega_d + i\zeta\omega_n$$
$$q_1 = p_1 - \omega_2 = (\omega_d - \omega_2) + i\zeta\omega_n \qquad q_2 = p_2 - \omega_2 = (-\omega_d - \omega_2) + i\zeta\omega_n \tag{24}$$

and the integral may be solved by applying equation (6) and letting α_1 correspond to p_1, α_2 to p_2, α_3 to q_1 and α_4 to q_2 and adopting equation (8) which results in the following four residues:

$$\text{residue at } \alpha_1 = \frac{e^{ip_1t}}{(p_1-p_2)(p_1-q_1)(p_1-q_2)} = \frac{e^{i(\omega_d+i\zeta\omega_n)t}}{(2\omega_d)(\omega_2)(2\omega_d+\omega_2)}$$
$$\text{residue at } \alpha_2 = \frac{e^{ip_2t}}{(p_2-p_1)(p_2-q_1)(p_2-q_2)} = \frac{e^{i(-\omega_d+i\zeta\omega_n)t}}{(-2\omega_d)(-2\omega_d+\omega_2)(\omega_2)}$$
$$\text{residue at } \alpha_3 = \frac{e^{iq_1t}}{(q_1-p_1)(q_1-p_2)(q_1-q_2)} = \frac{e^{i(\omega_d-\omega_2+i\zeta\omega_n)t}}{(-\omega_2)(2\omega_d-\omega_2)(2\omega_d)}$$
$$\text{residue at } \alpha_4 = \frac{e^{iq_2t}}{(q_2-p_1)(q_2-p_2)(q_2-q_1)} = \frac{e^{i(-\omega_d-\omega_2+i\zeta\omega_n)t}}{(-2\omega_d-\omega_2)(-\omega_2)(-2\omega_d)} \tag{25}$$

Summing the above four residues and substituting the result into equation (6) gives the following expression for the first integral of equation(23):

$$\int_{-\infty}^{\infty} \frac{d\omega_1\ e^{i\omega_1 t}}{(\omega_1-p_1)(\omega_1-p_2)(\omega_1+\omega_2-p_1)(\omega_1+\omega_2-p_2)} = \frac{\pi i}{(\omega_d)(\omega_2)(\omega_2+2\omega_d)(\omega_2-2\omega_d)} \times \tag{26}$$

$$\left\{(\omega_2-2\omega_d)\,e^{i(\omega_d+i\zeta\omega_n)t} - (\omega_2+2\omega_d)\,e^{i(-\omega_d+i\zeta\omega_n)t} + (\omega_2+2\omega_d)\,e^{i(\omega_d-\omega_2+i\zeta\omega_n)t} - (\omega_2-2\omega_d)\,e^{i(-\omega_d-\omega_2+i\zeta\omega_n)t}\right\}$$

The above expression may now be substituted into equation (23) to give the following expression only dependent upon ω_2:

$$y_2(t) = \frac{k_2}{m^3}\left(\frac{A}{2\pi}\right)^2 \frac{\pi i}{\omega_d}\int_{-\infty}^{\infty} \frac{d\omega_2\ e^{i\omega_2 t}}{(\omega_2-p_1)(\omega_2-p_2)(\omega_2)(\omega_2+2\omega_d)(\omega_2-2\omega_d)} \times \tag{27}$$

$$\left\{(\omega_2-2\omega_d)\,e^{i(\omega_d+i\zeta\omega_n)t} - (\omega_2+2\omega_d)\,e^{i(-\omega_d+i\zeta\omega_n)t} + (\omega_2+2\omega_d)\,e^{i(\omega_d-\omega_2+i\zeta\omega_n)t} - (\omega_2-2\omega_d)\,e^{i(-\omega_d-\omega_2+i\zeta\omega_n)t}\right\}$$

Observation of the above integral shows that there are two complex poles (at $\omega_2 = p_1$ and $\omega_2 = p_2$) and three poles on the real axis of the complex plane (at $\omega_2 = 0$, $\omega_2 = 2\omega_d$ and $\omega_2 = -2\omega_d$). If the contour is closed on the upper-half of the complex plane, these final three poles on the real axis will only contribute one-half to the overall integral, i.e.

$$I = 2\pi i\,(\text{res } \alpha_1 + \text{res } \alpha_2) + \pi i\,(\text{res } \alpha_3 + \text{res } \alpha_4 + \text{res } \alpha_5) \tag{28}$$

It transpires that the residues at α_3, α_4 and α_5 are all equal to zero and only the residues at α_1 and α_2 (corresponding to p_1 and p_2 respectively) are non-zero. These residues are given by:

$$\text{residue at } \alpha_1 =$$
$$\frac{\left\{(-\omega_d+i\zeta\omega_n)\,e^{i(2\omega_d+i2\zeta\omega_n)t} - (3\omega_d+i\zeta\omega_n)\,e^{i(i2\zeta\omega_n)t} + (3\omega_d+i\zeta\omega_n)\,e^{i(\omega_d+i\zeta\omega_n)t} - (-\omega_d+i\zeta\omega_n)\,e^{i(-\omega_d+i\zeta\omega_n)t}\right\}}{(2\omega_d)(\omega_d+i\zeta\omega_n)(3\omega_d+i\zeta\omega_n)(-\omega_d+i\zeta\omega_n)}$$
$$\text{residue at } \alpha_2 = \tag{29}$$
$$\frac{\left\{(-3\omega_d+i\zeta\omega_n)\,e^{i(i2\zeta\omega_n)t} - (\omega_d+i\zeta\omega_n)\,e^{i(-2\omega_d+i2\zeta\omega_n)t} + (\omega_d+i\zeta\omega_n)\,e^{i(\omega_d+i\zeta\omega_n)t} - (-3\omega_d+i\zeta\omega_n)\,e^{i(-\omega_d+i\zeta\omega_n)t}\right\}}{(-2\omega_d)(-\omega_d+i\zeta\omega_n)(\omega_d+i\zeta\omega_n)(-3\omega_d+i\zeta\omega_n)}$$

The above two residues may then be substituted into equation (28) followed by a large amount of tidying-up which eventually results in the following expression for the integral in equation (27):

$$I = \frac{\pi i}{(\omega_d)(\omega_n^2)(8\omega_d^2+\omega_n^2)}\times$$

$$\Big\{(-3\omega_d+i\zeta\omega_n)\,(-\omega_d+i\zeta\omega_n)\,e^{i(2\omega_d+i2\zeta\omega_n)t}+(3\omega_d+i\zeta\omega_n)\,(\omega_d+i\zeta\omega_n)\,e^{i(-2\omega_d+i2\zeta\omega_n)t}+$$

$$2\left(8\omega_d^2+\omega_n^2\right)e^{-2\zeta\omega_n t}-\left[\left(8\omega_d^2+\omega_n^2\right)+(3\omega_d+i\zeta\omega_n)\,(\omega_d+i\zeta\omega_n)\right]e^{i(\omega_d+i\zeta\omega_n)t}-$$

$$\left[\left(8\omega_d^2+\omega_n^2\right)+(-3\omega_d+i\zeta\omega_n)\,(-\omega_d+i\zeta\omega_n)\right]e^{i(-\omega_d+i\zeta\omega_n)t}\Big\} \tag{30}$$

This expression may be further simplified by pairing up complex exponentials to give the final expression for the integral in equation (27):

$$I = \frac{2\pi i}{(\omega_d)(\omega_n^2)}\left(e^{-2\zeta\omega_n t}-e^{-\zeta\omega_n t}\cos(\omega_d t)\right)+$$

$$\frac{2\pi i}{(\omega_d)(\omega_n^2)(8\omega_d^2+\omega_n^2)}\left(|B|e^{-2\zeta\omega_n t}\cos(2\omega_d t+\angle B)-|C|e^{-\zeta\omega_n t}\cos(\omega_d t+\angle C)\right) \tag{31}$$

where

$$B=(-3\omega_d+i\zeta\omega_n)(-\omega_d+i\zeta\omega_n)\qquad\text{and}\qquad C=(3\omega_d+i\zeta\omega_n)(\omega_d+i\zeta\omega_n) \tag{32}$$

Finally, the expression for $y_2(t)$ may be obtained by substituting the integral expression of equation (31) into equation (27) giving:

$$y_2(t)=\frac{A^2k_2}{2m^3\omega_d^2\omega_n^2}\left\{e^{-\zeta\omega_n t}\cos(\omega_d t)-e^{-2\zeta\omega_n t}\right\}$$

$$+\frac{A^2k_2}{2m^3\omega_d^2\omega_n^2(8\omega_d^2+\omega_n^2)}\left\{|C|e^{-\zeta\omega_n t}\cos(\omega_d t+\angle C)-|B|e^{-2\zeta\omega_n t}\cos(2\omega_d t+\angle B)\right\} \tag{33}$$

where B and C are as in equation (32). Examination of the above expression for $y_2(t)$ shows that it introduces three components. In addition to a decaying exponential component at the rate of $2\zeta\omega_n$ and a $2\zeta\omega_n$ decaying sinusoidal component with frequency $2\omega_d$, there is also a decaying sinusoidal component at the same frequency and rate of decay as the linear $y_1(t)$ component i.e. a $\zeta\omega_n$ decaying sinusoidal component with frequency ω_d. In the above expression, this component was split into two parts, for presentation purposes.

It is not difficult to imagine the effect of the exponential increase in complexity upon the $y_3(t)$ expression and therefore, due to considerations of space, the contour integral process for the $y_3(t)$ expression will not be explained with the same level of detail as the $y_2(t)$ expression previously. The $y_3(t)$ expression is obtained by substituting the expression for $H_3(\omega_1,\omega_2,\omega_3)$ given in equation (17) (taking advantage of ω_1, ω_2, ω_3 symmetry) into the third component of equation (19):

$$y_3(t)=\left(\frac{A}{2\pi}\right)^3\int_{-\infty}^{\infty}\int_{-\infty}^{\infty}\int_{-\infty}^{\infty}d\omega_1 d\omega_2 d\omega_3\;H_3(\omega_1,\omega_2,\omega_3)\;e^{i(\omega_1+\omega_2+\omega_3)t} \tag{34}$$

$$=\left(\frac{A}{2\pi}\right)^3\int_{-\infty}^{\infty}\int_{-\infty}^{\infty}\int_{-\infty}^{\infty}d\omega_1 d\omega_2 d\omega_3\;H_1(\omega_1+\omega_2+\omega_3)H_1(\omega_1)H_1(\omega_2)H_1(\omega_3)\left[2k_2^2H_1(\omega_1+\omega_2)-k_3\right]\;e^{i(\omega_1+\omega_2+\omega_3)t}$$

As with the $y_2(t)$ calculation, the H_1s may be written in polar form. The above expression may be split into two triple integrals, one which depends upon the cubic stiffness, k_3, and the other which depends upon the quadratic stiffness, k_2. This will make the :

$$y_3(t)=y_3^{k_3}(t)+y_3^{k_2}(t)=-\frac{k_3}{m^4}\left(\frac{A}{2\pi}\right)^3\int_{-\infty}^{\infty}\int_{-\infty}^{\infty}\int_{-\infty}^{\infty}\frac{d\omega_1 d\omega_2 d\omega_3\;e^{i(\omega_1+\omega_2+\omega_3)t}}{\text{Denominator}_1}$$

$$-\frac{2k_2^2}{m^5}\left(\frac{A}{2\pi}\right)^3\int_{-\infty}^{\infty}\int_{-\infty}^{\infty}\int_{-\infty}^{\infty}\frac{d\omega_1 d\omega_2 d\omega_3\;e^{i(\omega_1+\omega_2+\omega_3)t}}{\text{Denominator}_2} \tag{35}$$

where

$$\text{Denominator}_1 = (\omega_1-p_1)(\omega_1-p_2)(\omega_2-p_1)(\omega_2-p_2)(\omega_3-p_1)(\omega_3-p_2)(\omega_1+\omega_2+\omega_3-p_1)(\omega_1+\omega_2+\omega_3-p_2) \quad (36)$$

and

$$\text{Denominator}_2 = (\omega_1 - p_1)(\omega_1 - p_2)(\omega_2 - p_1)(\omega_2 - p_2)(\omega_3 - p_1)(\omega_3 - p_2)\times$$
$$(\omega_1 + \omega_2 + \omega_3 - p_1)(\omega_1 + \omega_2 + \omega_3 - p_2)(\omega_1 + \omega_2 - p_1)(\omega_1 + \omega_2 - p_2) \quad (37)$$

After following the same process as for $y_2(t)$, the following expression was calculated for the $y_3^{k_3}(t)$ component of equation (35):

$$y_3^{k_3}(t) = \frac{A^3 k_3}{32m^4(\zeta\omega_n)(\omega_d^3)(\omega_n^2)(12\omega_d^2 + 4\omega_n^2)}\times$$
$$\left\{|D|e^{-3\zeta\omega_n t}\cos(3\omega_d t + \angle D) + |E|e^{-3\zeta\omega_n t}\cos(\omega_d t + \angle E) + |F|e^{-\zeta\omega_n t}\cos(\omega_d t + \angle F)\right\} \quad (38)$$

where

$$D = 24\omega_d\zeta^2\omega_n^2 + i16\omega_d^2\zeta\omega_n - i8\zeta^3\omega_n^3$$
$$E = -96\omega_d^3 - 24\omega_d\zeta^2\omega_n^2 + i96\omega_d^2\zeta\omega_n + i24\zeta^3\omega_n^3$$
$$F = 96\omega_d^3 + i48\omega_d^2\zeta\omega_n + i24\zeta^3\omega_n^3 \quad (39)$$

Examination of equation (38) shows that three components are introduced in the $y_3(t)$ part of the impulse response due to the presence of a cubic stiffness, k_3, term. These components are a $3\zeta\omega_n$ decaying sinusoidal component with frequency $3\omega_d$, a $3\zeta\omega_n$ decaying sinusoidal component with frequency ω_d and a decaying sinusoidal component at the same frequency and rate of decay as the linear $y_1(t)$ component i.e. a $\zeta\omega_n$ decaying sinusoidal component with frequency ω_d. It is worth noting at this point that, if a classical Duffing oscillator ($k_2 = 0$, $k_3 \neq 0$) is being analysed, there will be no $2\zeta\omega_n$ components. These same components were reported in [4] although the perturbation analysis resulted in different pre-multipliers than those reported here

An even more involved process is required for the calculation of the $y_3^{k_2}(t)$ component of equation (35) which eventually leads to:

$$y_3^{k_2}(t) = \frac{A^3k_2^2|G|e^{-3\zeta\omega_n t}}{8m^5(\omega_d^3)(\omega_n^4)(3\omega_d^2+\omega_n^2)(8\omega_d^2+\omega_n^2)}\cos(3\omega_d t + \angle G)$$
$$+\frac{A^3k_2^2|H|e^{-2\zeta\omega_n t}}{2m^5(\omega_d^3)(\omega_n^4)(8\omega_d^2+\omega_n^2)}\cos(2\omega_d t + \angle H) + \frac{2A^3k_2^2\zeta e^{-2\zeta\omega_n t}}{m^5(\omega_d^2)(\omega_n^3)(8\omega_d^2+\omega_n^2)}$$
$$+\frac{A^3k_2^2|J|e^{-3\zeta\omega_n t}}{8m^5\zeta(\omega_d^3)(\omega_n^5)(8\omega_d^2+\omega_n^2)}\cos(\omega_d t + \angle J) - \frac{A^3k_2^2e^{-\zeta\omega_n t}}{4m^5\zeta(\omega_d^2)(\omega_n^5)}\cos(\omega_d t)$$
$$+\frac{A^3k_2^2|K|e^{-\zeta\omega_n t}}{8m^5\zeta(\omega_d^3)(\omega_n^5)(3\omega_d^2+\omega_n^2)(8\omega_d^2+\omega_n^2)}\cos(\omega_d t + \angle K) \quad (40)$$

where

$$G = 17\omega_d^3\zeta\omega_n - 7\omega_d\zeta^3\omega_n^3 + i6\omega_d^4 - i17\omega_d^2\zeta^2\omega_n^2 + i\zeta^4\omega_n^4$$
$$H = -4\omega_d\zeta\omega_n - i3\omega_d^2 + i\zeta^2\omega_n^2 - i\omega_n^2$$
$$J = 13\omega_d^3 + 2\omega_d\omega_n^2 + 5\omega_d\zeta^2\omega_n^2 - i9\omega_d^2\zeta\omega_n - i2\zeta\omega_n^3 - i\zeta^3\omega_n^3$$
$$K = 9\omega_d^5 - 32\omega_d^3\zeta^2\omega_n^2 + 3\omega_d^2\omega_n^2 + 7\omega_d\zeta^4\omega_n^4 - 5\omega_d\zeta^2\omega_n^4 + i27\omega_d^4\zeta\omega_n - i20\omega_d^2\zeta^3\omega_n^3 - i\zeta^3\omega_n^5 + i\zeta^5\omega_n^5 \quad (41)$$

Examination of equation (40) shows that a total of five components are introduced in the $y_3(t)$ part of the impulse response due to the presence of a quadratic stiffness, k_2, term. These components are $3\zeta\omega_n$ decaying sinusoidal components with frequency $3\omega_d$ and frequency ω_d, a $2\zeta\omega_n$ decaying sinusoidal component with frequency $2\omega_d$, a $2\zeta\omega_n$ decaying exponential component and a decaying sinusoidal component at the same frequency and rate of decay as the linear $y_1(t)$ component i.e. a $\zeta\omega_n$ decaying sinusoidal component with frequency ω_d. It is worth noting here that a k_3 nonlinearity is not required to introduce $3\zeta\omega_n$ components.

In the next section, the Volterra series expressions for the impulse response of a Duffing oscillator (symmetric and asymmetric) which have been derived in this section will be compared with the impulse response of the system obtained via numerical simulation.

5 Comparison between simulation and Volterra series expressions

In order to illustrate the effect of the including the $y_2(t)$ and $y_3(t)$ Volterra impulse response components in addition to the linear impulse response, a comparison with simulated data will now be presented. The system under consideration is the Duffing oscillator with equation of motion as given in equation (14) with the following parameters: mass, $m = 1$ kg, damping parameter, $c = 20$ N/(m/s), linear stiffness, $k_1 = 1 \times 10^4$ N/m, quadratic stiffness, $k_2 = 1 \times 10^7$ N/m^2 and cubic stiffness, $k_3 = 5 \times 10^9$ N/m^3. This means that the underlying linear system has an undamped natural frequency, $\omega_n = 100$ rad/s and a damping ratio, $\zeta = 0.1$. Three individual nonlinear systems were investigated: (1) a k_2 only system ($k_3 = 0$), (2) a k_3 only system ($k_2 = 0$) and (3) with both k_2 and k_3 parameters as above.

The three systems were simulated using Simulink® using a 4th-order Runge-Kutta integration scheme with a fixed step size of 0.0001s. The first one second of response was calculated in each case although the figures which follow of the displacement time responses will only focus on the first 0.2s in order to clearly highlight the differences between the simulated data and the Volterra series approximations.

The system with only a quadratic stiffness nonlinearity was simulated first and impulse response components $y_1(t)$, $y_2(t)$ and $y_3^{k_2}(t)$ were calculated by substituting the system parameter values into equations (20), (33) and (40) respectively. This was repeated for impulse excitation amplitudes ranging from $A = 0.01$N to $A = 0.09$N in steps of 0.01N. Note, increasing the level of forcing beyond $A = 0.09$N results in an unstable system due to the quadratic nonlinearity. Figures 2 and 3 display the simulated response and three Volterra responses for impulse amplitudes $A = 0.03$N and $A = 0.07$N respectively. At the lower level of forcing it may be seen that the inclusion of the $y_2(t)$ component gives a significantly better comparison with the simulated response than that from only considering the linear $y_1(t)$ component. Inclusion of the $y_3^{k_2}(t)$ component does not appear to be necessary at this level of forcing. However, when the forcing is increased to $A = 0.07$N, the $y_3^{k_2}(t)$ component does result in a significant improvement over the other two Volterra responses.

In order to provide a slightly more objective comparison between the different Volterra series approximations at different forcing levels, the root relative squared error between the Volterra response and simulated response over the first one second (N sample points) was calculated as follows:

$$\text{Root relative squared error} = 100\% \times \sqrt{\frac{\sum_{i=1}^{i=N} \left(y_{v_i}(t) - y_{s_i}(t)\right)^2}{\sum_{i=1}^{i=N} \left(\overline{y_s(t)} - y_{s_i}(t)\right)^2}} \tag{42}$$

where $y_{v_i}(t)$ and $y_{s_i}(t)$ are the i^{th} sample point of the the Volterra and simulated response signals respectively and $\overline{y_s(t)}$ is the mean value of the simulated response. Figure 4 plots the root relative error for the three Volterra approximations against impulse amplitude. It may be observed that inclusion of the $y_3^{k_2}(t)$ component results in a significant improvement over the linear response and $y_1(t) + y_2(t)$ response for all amplitudes but at the higher amplitudes the error increases dramatically for the three component response. It can also be noted that the $y_1(t) + y_2(t)$ response performs worse than the linear response for values of A greater than about 0.05N: this is largely due a greater phase lag from the two component response.

The system with only a cubic stiffness nonlinearity was simulated next. As the $y_2(t)$ component is zero for this system, only two Volterra responses are considered: the linear impulse response $y_1(t)$ and the sum of $y_1(t)$ and $y_3^{k_3}(t)$. These responses were calculated by substituting the system parameter values into equations (20)and (38). On this occasion, this was conducted for impulse excitation amplitudes ranging from $A = 0.01$N to $A = 0.15$N in steps of 0.01N. Figures 5 and 6 display the simulated response and two Volterra responses for impulse amplitudes $A = 0.07$N and $A = 0.12$N respectively. At $A = 0.07$N the inclusion of the $y_3^{k_3}(t)$ component has clearly improved matters but, at the higher level of forcing, the two component response results in an over-estimate of the simulated response, although its phase is an improvement on the linear response. Figure 7 shows the root relative error for the two Volterra approximations against impulse amplitude. It may be observed that inclusion of the $y_3^{k_3}(t)$ component results in a significant improvement over the linear response but there is a rapid increase in the error of the two component response after about 0.1N: the reason for this is that, at this level of forcing, the Volterra series approximation is approaching its limit of convergence.

The final system to be considered was the one with both quadratic and cubic stiffness elements. The impulse response components $y_1(t)$ and $y_2(t)$ were calculated by substituting the system parameter values into equations (20) and (33) respectively and the $y_3(t)$ component was calculated by substituting the parameter values into equations (40) and (38) and summing the two parts. As with the previous system,

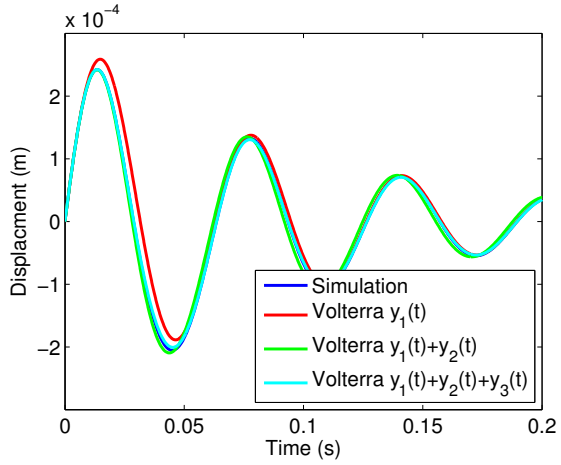

Fig. 2: Impulse response of k_2 only nonlinear system for impulse amplitude $A = 0.03$N

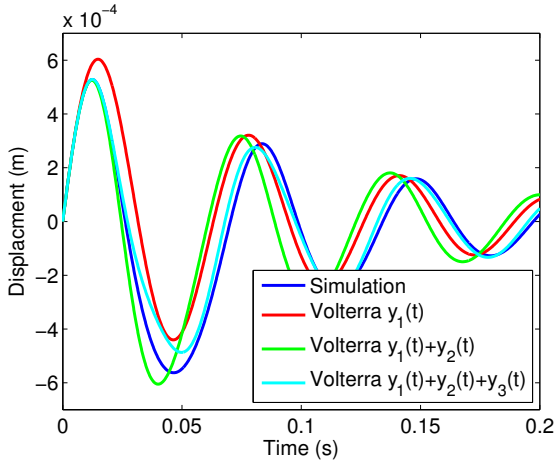

Fig. 3: Impulse response of k_2 only nonlinear system for impulse amplitude $A = 0.07$N

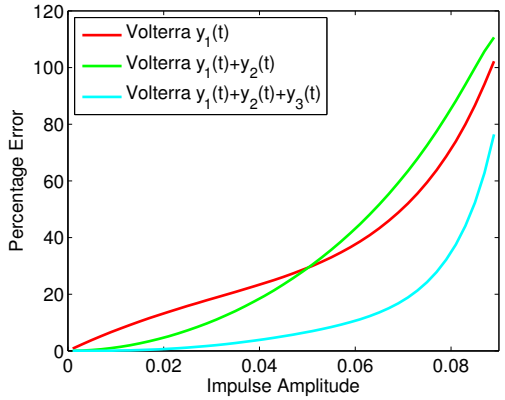

Fig. 4: Root relative squared error for Volterra impulse response approximations for k_2 only nonlinear system

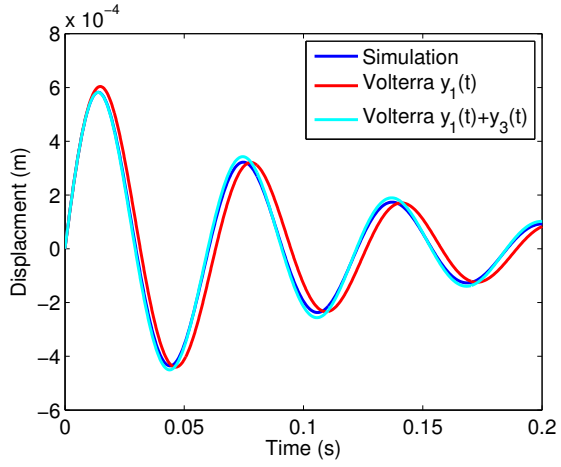

Fig. 5: Impulse response of k_3 only nonlinear system for impulse amplitude $A = 0.07$N

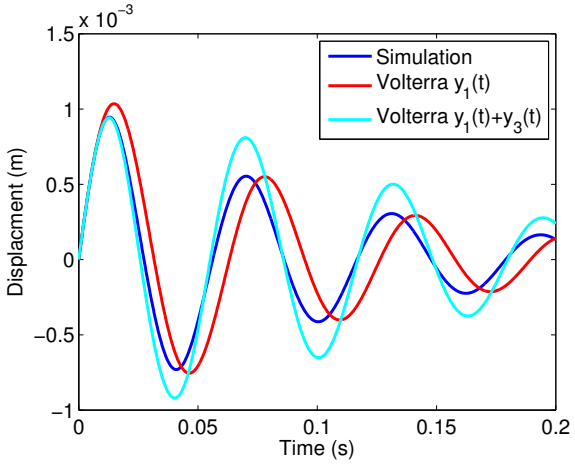

Fig. 6: Impulse response of k_3 only nonlinear system for impulse amplitude $A = 0.12$N

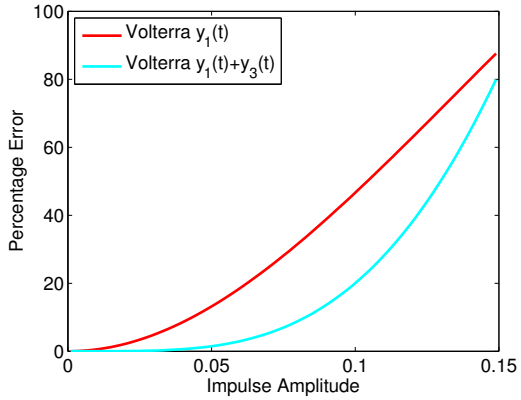

Fig. 7: Root relative squared error for Volterra impulse response approximations for k_3 only nonlinear system

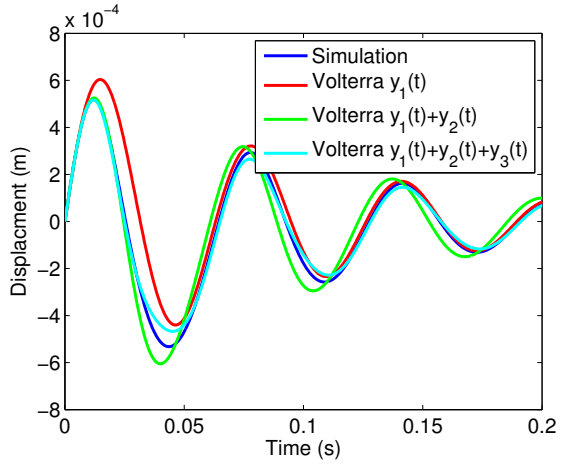

Fig. 8: Impulse response of k_2 and k_3 nonlinear system for impulse amplitude $A = 0.07$N

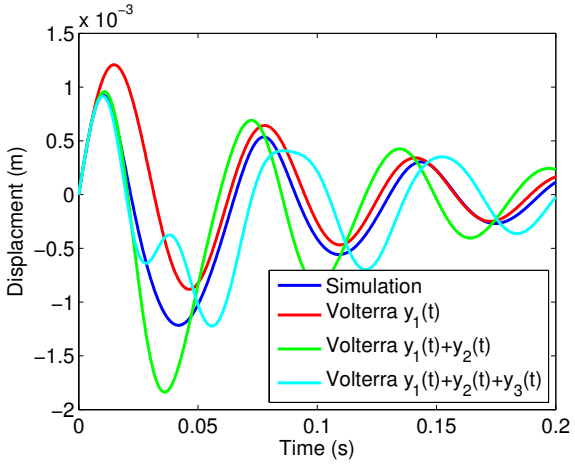

Fig. 9: Impulse response of k_2 and k_3 nonlinear system for impulse amplitude $A = 0.14$N

this was conducted for impulse excitation amplitudes ranging from $A = 0.01$N to $A = 0.15$N in steps of 0.01N. Figures 8 and 9 display the simulated response and two Volterra responses for impulse amplitudes $A = 0.07$N and $A = 0.14$N respectively. At $A = 0.07$N the inclusion of the $y_3(t)$ component has clearly improved matters but, at the higher level of forcing, the Volterra series is encountering issues with lack of series convergence: this is most pronounced around 0.04s in Figure 9 where it may be observed that the two component $(y_1(t) + y_2(t))$ response overestimates the amplitude but the addition of the $y_3(t)$ component has resulted in over-compensation. The situation does not improve as time increases with the three component response being as poor, if not worse, than the two component response, at this level of forcing. This perception is confirmed by the plot of the root relative errors for this system shown in figure 7. At levels of forcing below around $A = 0.1$N, the inclusion of the $y_2(t)$ component results in a reduced error when compared to the linear impulse response shows the root relative error for the two Volterra approximations against impulse amplitude. Inclusion of the $y_3(t)$ component significantly reduces this error further up to this level. As with the previous two systems, however, there is a pronounced increase in error of the three component response at higher levels, to such an extent that it actually returns the largest error after about $A = 0.13$N.

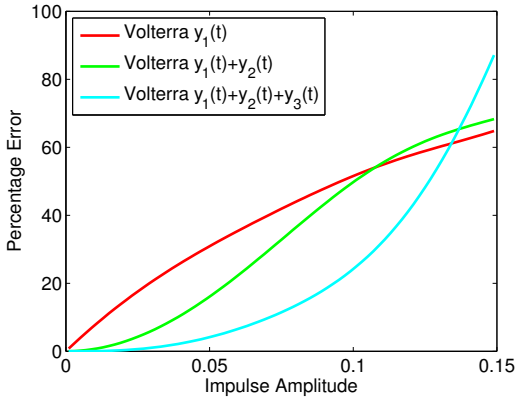

Fig. 10: Root relative squared error for Volterra impulse response approximations for k_2 and k_3 nonlinear system

6 Discussion and Conclusions

This paper was concerned with developing an analytical expression for the impulse response of nonlinear systems based around a framework provided by the Volterra series approximation for nonlinear system responses. The benefits of including the higher-order components was significant in terms of the reduction in error when compared to the simulated system. One of the most striking aspects of the work conducted relates to the rapid escalation in complexity of the Volterra series expressions and the effort required to obtain them. The authors have no plans to extend the calculation any further than the $y_3(t)$ component. Work, however, is ongoing to extending this study to multi degree of freedom nonlinear systems which will explain how multiple natural frequencies interact with one another when an impulse is applied to a more complex nonlinear system.

References

[1] Worden K and Manson G 1998 Random vibrations of a Duffing oscillator using the Volterra series *J. Sound Vibrat.* **217** 781–89

[2] Worden K and Manson G 1999 Random vibrations of a a multi-degree-of-freedom nonlinear system using the Volterra series *J. Sound Vibrat.* **226** 397–405

[3] Worden K and Manson G 2005 A Volterra series approximation to the coherence of the Duffing oscillator *J. Sound Vibrat.* **286** 529–47

[4] White R G 1973 Effects of non-linearity due to large deflections in the derivation of frequency response data from the impulse response of structures *J. Sound Vibrat.* **29(3)** 295–307

[5] Mohammad K 1990 Identification of the Characteristics of Non-linear Structures Ph.D Thesis: Heriot-Watt University

[6] Palm G and Poggio T 1977 The Volterra representation and the Wiener expansion: validity and pitfalls *SIAM J. App. Math.* **33** (2) 195–216

[7] Rugh W J 1981 *Nonlinear System Theory - The Volterra/Wiener Approach* (John Hopkins University Press)

[8] Barrett J F 1965 The use of Volterra series to find region of stability of a non-linear differential equation *Int. J. Control* **1** (3) 209–16

[9] Kreyszig E 1999 *Advanced Engineering Mathematics* (John Wiley & Sons)

[10] Goldhaber M Dispersion Relations *Theorie de la Particules Elementaire* (Paris: Hermann)

[11] Volterra V 1959 *Theory of Functionals and Integral equations* (New York: Dover Publications)

[12] Schetzen M 1980 *The Volterra and Wiener Theories of Nonlinear Systems* (New York: John Wiley Interscience Publication)

[13] Bedrosian E and Rice S O 1971 The output properties of Volterra systems driven by harmonic and Gaussian inputs *P. IEEE* **59** 1688–707